

# INTERNATIONAL SOCIETY FOR SOIL MECHANICS AND GEOTECHNICAL ENGINEERING



*This paper was downloaded from the Online Library of the International Society for Soil Mechanics and Geotechnical Engineering (ISSMGE). The library is available here:*

<https://www.issmge.org/publications/online-library>

*This is an open-access database that archives thousands of papers published under the Auspices of the ISSMGE and maintained by the Innovation and Development Committee of ISSMGE.*

*The paper was published in the proceedings of the 20<sup>th</sup> International Conference on Soil Mechanics and Geotechnical Engineering and was edited by Mizanur Rahman and Mark Jaksa. The conference was held from May 1<sup>st</sup> to May 5<sup>th</sup> 2022 in Sydney, Australia.*

# Mapping of liquefaction hazard for Lebanon: a macrozonation study

Cartographie des risques de liquéfaction pour le Liban : une étude de macrozonation.

**Graziella Sebaaly**

*PhD Candidate, Faculty of Engineering, Saint Joseph University, Beirut, Lebanon, graziella.sebaaly1@usj.edu.lb*

**Muhsin Elie Rahhal**

*Professor, Faculty of Engineering, Saint Joseph University, Beirut, Lebanon*

**Jean Pierre Seoud**

*CEO, Géotechnique et Structure Consultants, GSC sal, Beirut, Lebanon*

**ABSTRACT:** Mapping of liquefaction hazards in terms of probability is a key tool for risk assessment of natural disasters. Considering that Lebanon lies along an important seismic zone that accounts for the bulk of the seismic activity in the Eastern Mediterranean and a quaternary formation consisting mainly of sandy alluvium exists at its coast and locally in the internal area, liquefaction risk mapping at the country scale is important. In this study, Lebanon's macrozonation of liquefaction hazards is carried out in a GIS environment by adopting a data-driven method. The soil susceptibility to liquefaction is assessed by using the geospatial liquefaction model developed by Zhu et al. (2015). The mapping of the probability of liquefaction along the Lebanese territory for a seismic hazard of a return period of 475 years shows a high probability of liquefaction among some coastal cities. A lower probability of liquefaction is obtained as we move from the coastal area except for the quaternary formation around Nahr El Litani, showing a probability of liquefaction higher than 20% (high risk).

**RÉSUMÉ :** La cartographie des risques de liquéfaction en termes de probabilité est un outil clé pour l'évaluation des risques de catastrophes naturelles. Considérant que le Liban se situe le long d'une importante zone sismique qui représente l'essentiel de l'activité sismique en Méditerranée orientale et qu'une formation quaternaire constituée principalement d'alluvions sableuses existe sur sa côte et localement dans la zone interne, la cartographie des risques de liquéfaction à l'échelle du pays est importante. Dans cette étude, la macrozonation des risques de liquéfaction au Liban est réalisée dans un environnement GIS en adoptant une méthode basée sur les données. La sensibilité du sol à la liquéfaction est évaluée à l'aide du modèle de liquéfaction géospatiale développé par Zhu et al. (2015). La cartographie de la probabilité de liquéfaction le long du territoire libanais pour un aléa sismique d'une période de retour de 475 ans montre une forte probabilité de liquéfaction dans certaines villes côtières. Une probabilité de liquéfaction plus faible est obtenue lorsque nous nous déplaçons de la zone côtière à l'exception de la formation quaternaire autour de Nahr El Litani, montrant une probabilité de liquéfaction supérieure à 20% (risque élevé).

**KEYWORDS:** liquefaction, mapping, risk, macrozonation, GIS.

## 1 INTRODUCTION

Liquefaction hazard mapping gains its importance from the fact that ground failure generated by liquefaction have been a major cause of damage during past earthquakes (Chile 2010, New Zealand 2010 and 2011, Japan 2011). Therefore, a liquefaction mapping is an important key for risk assessment of natural disasters. The evaluation of soil liquefaction potential is mostly based on geotechnical data obtained from in-situ testing or laboratory testing for a specific location. Many methods have been developed to calculate the safety factor against liquefaction including (Seed and Idriss 1971), (Youd, Idriss, et al. 2001) and (Boulanger and Idriss 2014). Additionally, the liquefaction potential index was introduced by (Iwasaki, et al. 1978). It predicts the performance of the whole soil column by combining the effect of the depth, thickness, and severity of liquefaction occurrence. It is the most used index for liquefaction risk mapping.

However, liquefaction mapping on a large scale is a challenging task. Consequently, developing a model that uses broadly available data seems quite impossible to a certain point. Few models were developed with the purpose to generate liquefaction risk maps ( Youd and Perkins, Mapping liquefaction-induced ground failure potential 1978), (Zhu, Daley, et al. 2015) and (Zhu, Baise and Thompson 2017)).

Considering that Lebanon lies across an important seismic zone and that quaternary formation exist among its coastal area and within its internal areas, the country has areas with high susceptibility of liquefaction. Liquefaction mapping is established using the geospatial liquefaction model developed by (Zhu, Daley, et al. 2015). The model is a data-driven method based on geological, geomorphological, hydrological data and for a given level of expected ground shaking.

The analysis was carried out in a GIS (Geographic Information System) environment. The maps are computed for a return period of 475 years of ground shaking (10% probability of exceedance in 50 years).

## 2 METHODOLOGY

The model defined by (Zhu, Daley, et al. 2015) is adopted in this study. It computes the probability of liquefaction based on geospatial, hydrological, and seismic variables. It is calculated using the following mathematical model:

$$P_L = \frac{1}{1+e^{-x}} \quad (1)$$

Where  $x$  is a linear function of the explanatory variables. Two models were defined: global and regional models. The regional

model is developed for coastal sedimentary areas. However, the global model is not limited to coastal areas. Considering that based on the geology of Lebanon, potentially liquefiable soil exists in both coastal and inland areas, both models were used in this study depending on the designated area location.

For the global model:

$$x = 24.1 + 2.07 \ln(PGA_M) + 0.355CTI - 4.784 \ln(V_{s30}) \quad (2)$$

For the regional model:

$$x = 15.83 + 1.443 \ln(PGA_M) + 0.136CTI - 9.759 ND - 2.764 \ln(V_{s30}) \quad (3)$$

The above models englobe the soil saturation represented by compound topographic index (CTI) and the normalized distance (ND), the soil density represented by the average shear wave velocity in the upper 30m ( $V_{s30}$ ) and the normalized distance (ND), and the earthquake loading represented by the magnitude weighted peak ground acceleration ( $PGA_M$ ).

The obtained probability of liquefaction from the above defined models is categorized into five classes as defined by (Zhu, et al., 2015) and shown in table 1.

Table 1. Liquefaction risk classification by Zhu et al. (2015)

Probability of Liquefaction (PL)	Liquefaction Risk
$PL < 0.01$	Very Low
$0.01 < PL \leq 0.03$	Low
$0.03 < PL \leq 0.08$	Medium
$0.08 \leq PL \leq 0.2$	High
$0.2 < PL \leq 1$	Very high

### 3 GIS DATABASE

In order to implement the (Zhu, Daley, et al. 2015) model, a collection of data within a GIS platform was conducted. The following data were collected, calculated, and stored as raster files.

#### 3.1 Geological data

The first step consists of differentiating between soil and rock. Figure 1 shows the geological map established by L.Dubertret (1955) on a scale 1/200,000. This map was based on larger-scale geological maps (scale 1/50,000) prepared by L. Dubertret and his collaborators. In summary, the geological formations of Lebanon can be summarized by five main geological formations: Jurassic (thick shell limestone), Lower Cretaceous (Sandstones overlain by thick marine limestone), Upper Cretaceous (chalks and limestone), Miocene (limestone on coasts, conglomerates, and lake deposits in Bekaa) and Quaternary (alluviums, dunes and lake deposits). Based on the considered geological maps, the quaternary formation consisting of marine deposits, river terraces, dunes and alluvial deposits was delimited. The Quaternary formation occupies 11% of the total area of Lebanon. Despite the relatively small percentage occupied by the quaternary formation, the importance of this liquefaction susceptibility study resides in the fact that the quaternary formations are located within the most populated areas in Lebanon. Additionally, many land reclamation projects took place along the coast of Lebanon (within the capital Beirut, and along the northern area of Beirut) consisting in some areas of rocky fill and of soil fill in others. Based on existing soil investigation in such areas, they were categorized as soil or rock depending on the depth and the nature of the fill material. Therefore, a soil/rock separation was executed on the territory of Lebanon. Additionally, considering that both global and regional models were used, a separation was implemented between the quaternary formation located on the

coastal area and the one located inland.

While the above geological information separates the soil and rock formations, the density of a soil factor is a key factor in determining the occurrence of liquefaction. The average shear wave velocity down to 30m of depth ( $V_{s30}$ ) was introduced as a proxy for the soil density. The global topographic slope based  $V_{s30}$  map was downloaded from <https://earthquake.usgs.gov/data/vs30/>. Based on simple and natural correlation between topography and surficial geology correlation, these maps were developed by (Wald & Allen, 2007) by deriving the mapping of  $V_{s30}$  anywhere on the globe from the topographic scale. Lebanon boundary clipped map of the shear wave velocity was stored in the GIS data as a raster file. A second proxy for soil density exclusively for the coastal areas is the normalized distance (ND). It is defined as the distance to the coast divided by the sum of the distance to coast and the distance to the inland edge of the sedimentary edge. The normalized distance is an indication of the age of the sediments which is in relation to the distance to the coast. The closer to the coast, the younger and looser the sediments are. The normalized distance raster is calculated within GIS using the spatial analyst feature.

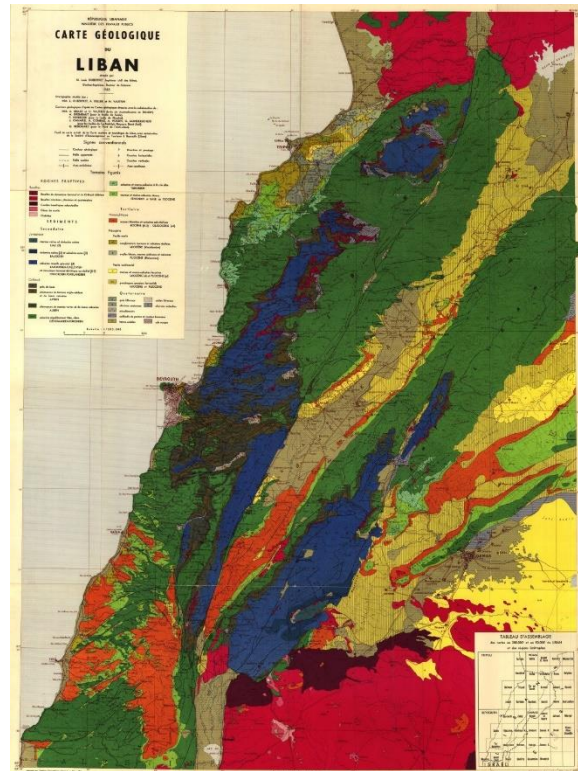


Figure 1. Geological Map of Lebanon established by L.Dubertret (1955)

#### 3.2 Hydrological data

The hydrological data has a purpose to represent the degree of saturation. For the coastal area, the normalized distance is a proxy attributing to the degree of saturation. The second proxy that is used in both models is the compound topographic index (CTI). The CTI known as a steady-state index is defined as the natural logarithm of the ratio of contributing area to the tangent slope (Moore, Grayson and Ladson 1991). To obtain the values of CTI, the Digital Elevation Model (DEM) from Shuttle Radar Topography Mission (SRTM) was geo-processed through the calculation of two raster files: the flow accumulation and the slope.

### 3.3 Seismic data

In addition to the geological and hydrogeological data defined above, seismic data were gathered and geo-processed. The earthquake loading is defined in the model in terms of magnitude weighted peak ground acceleration ( $PGA_M$ ). The  $PGA_M$  accounts for the effect of the earthquake duration by multiplying the PGA by the magnitude weighting factor (MWF). MWF is the inverse of the magnitude scaling factor (MSF) which is defined in (Youd, Idriss, et al. 2001) as a function of the moment magnitude (M).

Taking into account the location of Lebanon across an estimated 1000 km long fault which extends from the seafloor spreading in Red Sea to the Taurus mountains in southern Turkey, Lebanon is considered at a high seismic risk. The above-mentioned fault is known as the Levant or Dead Sea fault system accounts for the bulk of seismic activity in the Eastern Mediterranean. The map for peak ground acceleration with a 10% probability of exceedance in 50 years as established by (Huijjer, Harajli and Sadek 2016) was used as a starting point for dynamic loading definition across Lebanon.

## 4 MAPPING OF LIQUEFACTION RISK ACROSS LEBANON

Both models were applied based on the location of the quaternary formation (coastal or inland). The calculations were executed using a GIS-based methodology by applying a geospatial analysis. Each parameter is computed for a specific cell of the designated raster file. The resolution of the map is dictated by the largest resolution of the above-detailed input data.

The organigramme in figure 2 shows the followed procedure. Having all data stored as raster files, the probability of liquefaction is computed by applying the models defined by (Zhu, Daley, et al. 2015) with reference to a return period of 475 years.

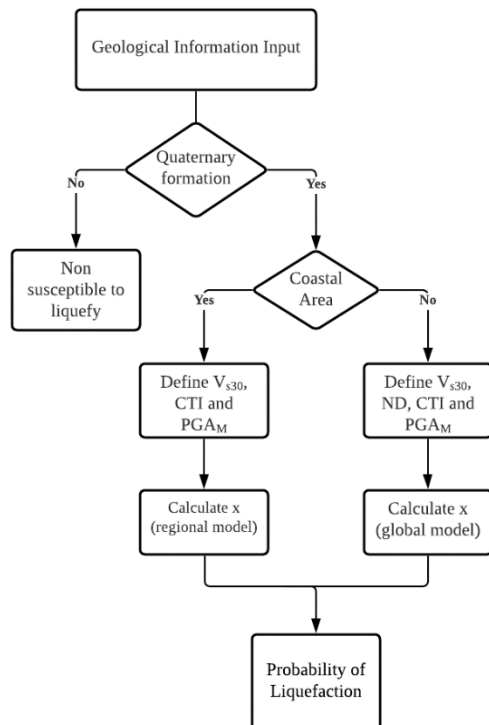


Figure 2. Calculations steps for liquefaction mapping along Lebanon

## 5 RESULTS

The resulting map of the liquefaction mapping along Lebanon for a return period of 475 years is shown in figure 3. The areas in grey were excluded from the calculation given that they belong to geological formations not susceptible to liquefy. The liquefaction risk is classified based on the probability of liquefaction as defined by (Zhu, et al., 2015) (table 1).

A high probability of liquefaction was interpreted among coastal cities such as the Capital Beirut, cities to the north of Beirut such as Antelias and Dbayeh, Tripoli and Saïda. Along the coastal cities, the probability of liquefaction decreases as moving far from the coastal line. This is related to the fact that as moving far from the coast, the groundwater is encountered at a deeper depth and therefore the saturation level decreases. A close up for Beirut city and to the northern of the city is shown in figure 4.

On the other hand, for the inland areas, the quaternary formation located around Nahr el Litani shows a high risk of liquefaction (probability of liquefaction higher than 20%). Similar to coastal area, the probability of liquefaction decreases as moving away from the river limit.

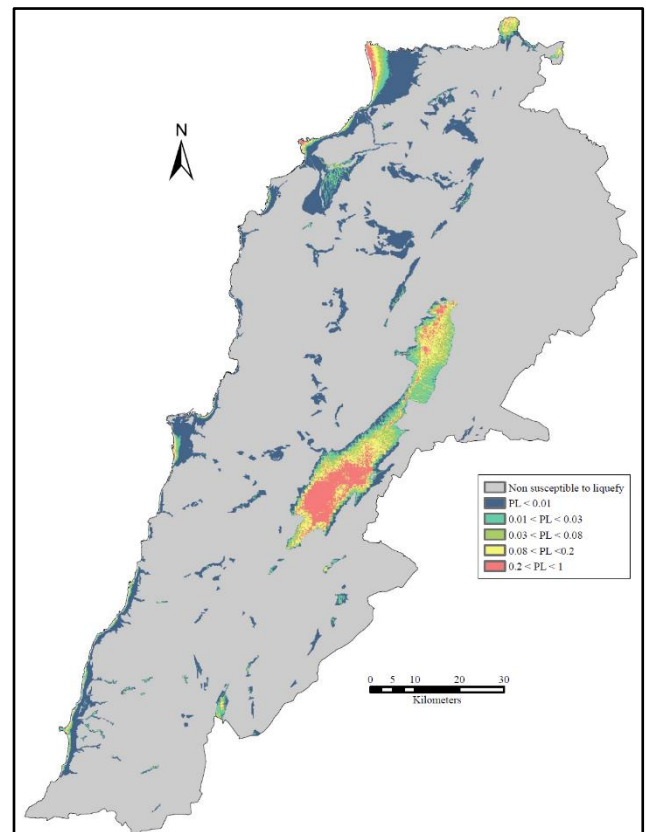


Figure 3. Map showing the liquefaction probability of Lebanon computed using (Zhu, et al., 2015) model for a return period of 475 years.



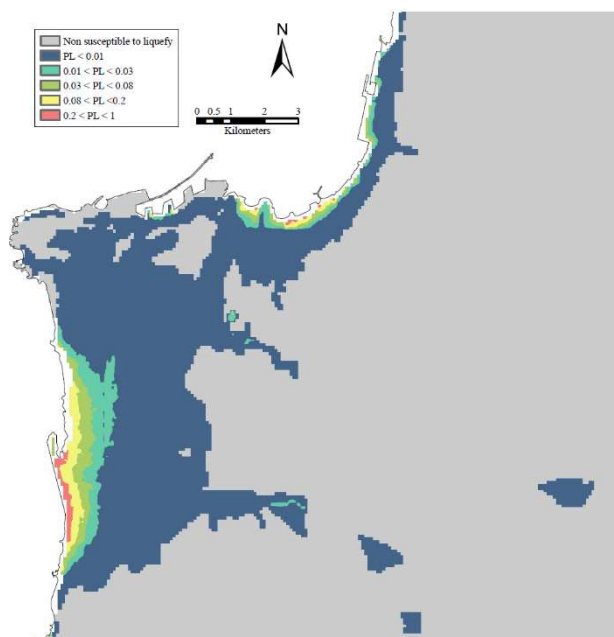


Figure 4. Close up Map showing the liquefaction probability of Beirut and the north of the city computed using (Zhu, et al., 2015) model for a return period of 475 years.

Among the quaternary formation, the distribution of the liquefaction risk classes is shown in form of a pie chart as shown in figure 5. Half of the quaternary formation presents a very low liquefaction risk with the calculated probability of liquefaction lower than 1%. The remaining areas are distributed almost equally between the other classes of liquefaction risks.

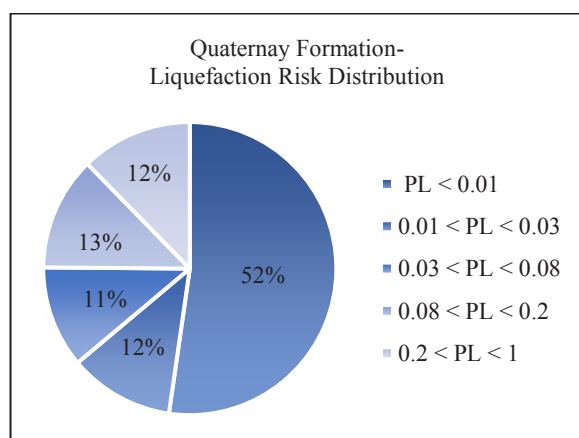


Figure 5. Pie chart showing the distribution of liquefaction risk classes among the quaternary formation.

## 6 CONCLUSIONS

In this study, an assessment of liquefaction was executed at the country scale. The mapping of the liquefaction risk of Lebanon based on the model defined by (Zhu, et al. 2015) adopting a data-driven method.

The mapping of the probability of liquefaction along the Lebanese territory for a seismic hazard of a return period of 475 years was carried out in a GIS environment using both global and regional models. The resulting map shows that half of the quaternary areas have a very low liquefaction risk, and the remaining areas are distributed almost equally between the other classes of liquefaction risks. Despite that, the importance of this mapping resides in the fact that most populated coastal cities are within areas of a very high risk of liquefaction.

A liquefaction mapping at a city scale based on geotechnical

field tests such as standard penetration test and cone penetration will be carried out in order to validate or redefine the obtained maps.

## 7. REFERENCES

- Boulanger, R. W., and I. M. Idriss. 2014. "CPT and SPT - Based liquefaction triggering procedures." Report No. UCD/CGM-10/01, April 2014, Center for Geotechnical Modeling - Department of Civil and Environmental Engineering, College of Engineering - University of California, Davis, USA.
- Huijter, C., M. Harajli, and S. Sadek. 2016. "Re-evaluation and updating of the seismic hazard of Lebanon." *J. Seismol* 233-250.
- Iwasaki, T., F. Tatsuoka, K. Tokida, and S. Yasuda. 1978. "A practical method for assessing soil liquefaction potential based on case studies at various sites in Japan." *2nd International Conference on Microzonation for Safer Construction*. New York: Amer. Society of Civil Eng. 885-896.
- Moore, I., R. Grayson, and A. Ladson. 1991. "Digital Terrain Modelling: A review of Hydrological, Geomorphological, and Biological Applications." *Hydrological Processes* 5: 3-30.
- Seed, H. B., and I. M. Idriss. 1971. "Simplified procedure for evaluating soil liquefaction potential." *Journal of the Soil Mechanics and Foundation Division (ASCE)* (97(9)): 1249-73.
- Wald, D J, and T I Allen. 2007. "Topographic slope as a proxy for seismic site conditions and amplification." *Bull Seismol Soc Am* 97 1379-1395.
- Youd, T. L., and D. M. Perkins. 1978. "Mapping liquefaction-induced ground failure potential." *Journal of the Geotechnical Engineering Division* GT4 (104): 433-446.
- Youd, T. L., I. M. Idriss, R. D. Andrus, I. Arango, G. Castro, J. T. Christian, R. Dobry, et al. 2001. "Liquefaction resistance of soils: summary report from the 1996 NCEER and 1998 NCEER/NSF workshops on evaluation of liquefaction resistance of soils." *Journal of Geotechnical and Geoenvironmental Engineering (ASCE)* 127 (10): 817-833.
- Zhu, J., L. G. Baise, and E. M. Thompson. 2017. "An updated geospatial liquefaction model for global application." *Bulletin of the Seismological Society of America* 107 (3): 1365-1385.
- Zhu, J., D. Daley, L. Baise, E. Thompson, D. Wald, and K. Knudsen. 2015. "A Geospatial Liquefaction Model for Rapid Response and Loss Estimation." *Earthquake Spectra* 31(3): 1813-1837.